We are IntechOpen, the world's leading publisher of Open Access books Built by scientists, for scientists

4,800
Open access books available

122,000
International authors and editors

135M
Downloads

Our authors are among the

154
Countries delivered to

TOP 1%
most cited scientists

12.2%
Contributors from top 500 universities

CLARIVATE ANALYTICS BOOK CITATION INDEX INDEXED

WEB OF SCIENCE™

Selection of our books indexed in the Book Citation Index in Web of Science™ Core Collection (BKCI)

Interested in publishing with us?
Contact book.department@intechopen.com

Numbers displayed above are based on latest data collected.
For more information visit www.intechopen.com

Chapter 3

Laser Beam Propagation through Oceanic Turbulence

Zhiqiang Wang, Lu Lu, Pengfei Zhang, Chunhong Qiao, Jinghui Zhang, Chengyu Fan and Xiaoling Ji

Additional information is available at the end of the chapter

http://dx.doi.org/10.5772/intechopen.76894

Abstract

Using a recently proposed model for the refractive index fluctuations in oceanic turbulence, optical beam propagation through seawater is explored. The model provides an accurate depiction of the ocean through the inclusion of both temperature and salinity fluctuations to the refractive index. Several important statistical characteristics are explored including spatial coherence radius, angle-of-arrival fluctuations, and beam wander. Theoretical values of these parameters are found based on weak fluctuation theory using the Rytov method. The results presented serve as a foundation for the study of optical beam propagation in oceanic turbulence, which may provide an important support for further researches in applications for underwater communicating, imaging, and sensing systems.

Keywords: oceanic turbulence, laser beam, spatial coherence radius, angle-of-arrival fluctuations, beam wander

1. Introduction

The study of optical wave propagation through random media is a perpetually important topic for its many applications in the atmosphere and the ocean. Random fluctuations in the index of refraction cause beam spreading (beyond that due to pure diffraction), loss of spatial coherence, random wandering of the instantaneous beam center, and random fluctuations in the irradiance and phase [1]. The index of refraction fluctuations, generally referred to as optical turbulence, is one of the most significant quantities in optical wave propagation. For different random media, there are some differentiations among the index of refraction fluctuations. The index of refraction of atmosphere is primarily caused by fluctuating temperature. The

refraction index in seawater is induced not only by temperature fluctuations but also by fluctuations of salinity. Changes in the optical signal due to absorption or scattering by molecules or particles are not considered here. Under the assumption of a statistically homogeneous and isotropic ocean, the power spectrum of oceanic turbulence is determined by fluctuations of refraction index.

With the development of underwater optical communications, imaging, sensor, and laser radar, it is indispensable to investigate the propagation behavior of laser beams through water medium. Knowledge of beam spreading is extremely important in a free space optics (FSO) communications link because it determines the loss of power at the receiver. The spatial coherence radius defines the effective receiver aperture size in a heterodyne detection system [1]. To the coherence degradation of laser beams, the spatial coherence radius can also be described as the strength of oceanic turbulence. Angle-of-arrival (AOA) fluctuations of an optical wave in the plane of the receiver aperture are associated with image jitter (dancing) in the focal plane of an imaging system [1] so that it plays a critical role in beam wave propagation applications such as imaging, lasercom, and other related areas. Movement of the short-term beam instantaneous center (or "hot spot") is commonly called beam wander [1]. Beam wander is an important propagation characteristic of laser beams, which determines their utility for practical applications, such as laser communication [2, 3] and global quantum communication [4].

In this chapter, Section 2 describes a brief introduction of oceanic turbulence including the power spectrum and several significant oceanic parameters. The spatial coherence radius of a plane wave and a spherical wave propagating through oceanic turbulence has been investigated in Section 3, which are valid in both weak and strong fluctuations. Section 4 describes the angle-of-arrival fluctuations for plane- and spherical-wave models of oceanic turbulence. Based on the oceanic power spectrum, the beam wander effect with analytical and numerical methods in weak fluctuation theory is shown in Section 5. These results may provide an inroad for understanding laser beam propagation through oceanic turbulence, and the theoretical findings may provide an important support for further researches in applications for underwater communicating, imaging, and sensing systems.

2. Nature of oceanic turbulence

Turbulence is a random, three-dimensional motion with the velocity and vorticity irregularly distributed in time and space [5]. In general, turbulence is accepted to be an energetic, rotational, and eddying state of motion that results in the dispersion of material and the transfer of momentum, heat, and solutes at rates far higher than those of molecular processes alone [6]. It is characterized by an energy transfer from large to small scales where the dissipation of kinetic energy is taking place [5]. Oceanic motions are constrained to flow along density surfaces by the Earth's rotation and the density stratification. In the upper ocean, microscale turbulence is generated by surface winds, air-sea cooling, or evaporation. In the ocean interior, microscale turbulence develops when internal waves develop strong shears and overturn and

break, much like surface gravity waves [7]. These breaking events play a fundamental role in the ocean circulation, because they mix the densest waters at the ocean bottom with the lighter waters above, thereby allowing the densest waters to come back to the surface [7]. Much of the turbulence induced in benthic boundary layers is driven by external processes resulting from the fluxes of buoyancy and momentum through the nearby boundary, such as a tidally driven current, geothermal heat flux, and so on [6]. They are driven by sources of energy outside the benthic boundary layer itself [6].

2.1. Power spectrum of oceanic turbulence

Since the power spectrum of oceanic turbulence proposed in 2000 [8], there has been remarkable interest in the study of propagation characteristics using laser beams in seawater. The power spectrum of oceanic turbulence has been simplified for homogeneous and isotropic water media [9], which is applicable for isothermal water [10]. When the eddy thermal diffusivity and the diffusion of salt are assumed to be equal, the power spectrum for homogeneous and isotropic oceanic water is given by the expression [11].

$$\Phi_n(\kappa) = 0.388 \times 10^{-8} \varepsilon^{-1/3} \kappa^{-11/3} \left[1 + 2.35(\kappa\eta)^{2/3}\right] \frac{\chi_T}{w^2} \left(w^2 e^{-A_T\delta} + e^{-A_S\delta} - 2we^{-A_{TS}\delta}\right), \quad (1)$$

where ε is the rate of dissipation of kinetic energy per unit mass of fluid ranging from about $10^{-10}\mathrm{m}^2/\mathrm{s}^3$ in the abyssal ocean to $10^{-1}\mathrm{m}^2/\mathrm{s}^3$ in the most actively turbulent regions. χ_T is the rate of dissipation of mean-squared temperature and has the range $10^{-4}\mathrm{K}^2/\mathrm{s}$–$10^{-10}\mathrm{K}^2/\mathrm{s}$, w defines the ratio of temperature and salinity contributions to the refractive index spectrum, which varies in the interval $[-5, 0]$, with -5 and 0 corresponding to dominating temperature-induced and salinity-induced optical turbulences, respectively [11]. In addition, η is the Kolmogorov microscale (inner scale), and $A_T = 1.863 \times 10^{-2}$, $A_S = 1.9 \times 10^{-4}$, $A_{TS} = 9.41 \times 10^{-3}$, $\delta = 8.284(\kappa\eta)^{4/3} + 12.978(\kappa\eta)^2$ [11].

2.2. Oceanic parameters

In this section, the abovementioned important parameters should be presented in detail that will benefit to more accurately comprehend the oceanic turbulence. In particular, the four significant parameters, such as the rate of dissipation of kinetic energy per unit mass of fluid, the rate of dissipation of mean-squared temperature, the Kolmogorov microscale, and the ratio of temperature and salinity contributions to the refractive index spectrum, will be mainly involved in the following subsections.

2.2.1. The rate of dissipation of kinetic energy per unit mass

The rate of dissipation of the kinetic energy of the turbulent motion per unit mass of fluid through viscosity to heat is usually denoted by ε, which can be expressed as [6].

$$\varepsilon = (v/2) < s_{ij} s_{ij} > \quad (2)$$

where v is the kinematic viscosity, the tensor s_{ij} is given by $s_{ij} = \left(\partial u_i/\partial x_j + \partial u_j/\partial x_i\right)$, $(i, j = 1, 2, 3)$, the velocity is written as $\vec{u} = u_1\ \vec{\mathrm{i}} + u_2\ \vec{\mathrm{j}} + u_3\ \vec{\mathrm{k}}$, here $\left(\vec{\mathrm{i}}, \vec{\mathrm{j}}, \vec{\mathrm{k}}\right)$ is the unit vector of a Cartesian coordinate system.

Recorded $u_1 = p$, $u_2 = q$, $u_3 = u$, $x_1 = x$, $x_2 = y$ and $x_3 = z$ in this section, for isotropic turbulence, the mean-squared gradients of velocity are equal (i.e., $\partial u_1/\partial x_1 = \partial u_2/\partial x_2 = \partial u_3/\partial x_3$), and which can be written as $\partial u/\partial z$ in vertical direction so that Eq. (2) reduces to the much simpler one [6].

$$\varepsilon = (15/2)v\left\langle (\partial u/\partial z)^2 \right\rangle \tag{3}$$

2.2.2. The rate of dissipation of mean-squared temperature

The effect of turbulence on the fluid temperature field can be described as the rate of dissipation of mean-squared temperature [6],

$$\chi_T = 2\kappa_T < (\partial T'/\partial x)^2 + (\partial T'/\partial y)^2 + (\partial T'/\partial z)^2 > \tag{4}$$

where κ_T is the eddy diffusion coefficients of heat, $\partial T'/\partial x$, $\partial T'/\partial y$ and $\partial T'/\partial z$ are the mean-squared gradients of temperature in three orthogonal coordinates.

In isotropic turbulence when the mean-squared gradients of temperature are the same in all directions, so that the rate of dissipation of mean-squared temperature becomes [6].

$$\chi_T = 6\kappa_T < (\partial T'/\partial z)^2 > \tag{5}$$

It is noted that the rate of dissipation of mean-squared salinity, χ_S, is defined similarly, but is harder to determine accurately because of problems in measuring salinity changes over small distances [6].

2.2.3. Kolmogorov microscale

The turbulent flow contains eddies of various sizes, and the energy is transferred from larger eddies to smaller eddies until it is drained out by viscous dissipation. Kolmogorov's hypothesis asserts that for large Reynolds numbers (i.e., inertial subrange), the small-scale structure of turbulence is statistically steady, isotropic, and locally homogeneous, and independent of the detailed structure of the large-scale components of turbulence [12]. Kolmogorov microscale is the smallest scale in turbulent flow. At the Kolmogorov scale, viscosity dominates and the turbulent kinetic energy is dissipated into heat. The length scale of the turbulent motions at which viscous dissipation becomes important must depend on factors that provide measures of the turbulent motion and of its viscous dissipation [6]. Kolmogorov length scale [13].

$$\eta = \left(v^3/\varepsilon\right)^{1/4} \tag{6}$$

where a range of η from about 6×10^{-5} m in very turbulent regions to 0.01 m in the abyssal ocean [6].

2.2.4. The ratio of temperature and salinity contributions to the refractive index spectrum

The parameter w is the ratio of temperature and salinity contributions to the refractive index spectrum given by

$$w = \frac{\alpha(\partial T/\partial z)}{\beta(\partial S/\partial z)} \tag{7}$$

where $\alpha = 2.6 \times 10^{-4}$liter/deg, $\beta = 1.75 \times 10^{-4}$liter/gram, $\partial T/\partial z$ and $\partial S/\partial z$ are, respectively, the gradients of mean temperature and salinity between the top and bottom boundaries of domain on the vertical coordinate [8].

3. Spatial coherence radius

When one coherent optical wave propagates through a random medium, various eddies impress a spatial phase fluctuation on the wave front with an imprint of the scale size [1]. The accumulation of such fluctuations on the phase leads to a reduction in the "smoothness" of the wave front [1]. Hence, turbulent eddies further away experience a smoothness of the wave front only on the order of the transverse spatial coherence radius, which Andrews and Phillips denote by ρ_0 [1]. After a wave propagates a sufficient distance, only those turbulent eddies on the order of ρ_0 or less are effective in producing further spreading and amplitude fluctuations on the wave [1]. Except for predicting random medium-induced beam spreading through the mean irradiance, the mutual coherence function (MCF) is also used to predict the spatial coherence radius of the wave at the receiver pupil plane. Obtained from the MCF, the spatial coherence radii of plane wave and spherical wave are, respectively, deduced in this section.

3.1. Plane wave

Under Rytov approximation, the wave structure function (WSF) of a plane wave propagating through isotropic and homogeneous turbulence is defined by [1].

$$D_{\mathrm{pl}}(\boldsymbol{\rho}, L) = 8\pi^2 k^2 L \int_0^\infty [1 - J_0(\kappa\rho)]\Phi_n(\kappa)\kappa \mathrm{d}\kappa, \tag{8}$$

where k is the optical wave number related to the wavelength λ by $k = 2\pi/\lambda$, L is the path length, κ is the magnitude of spatial wave number, ρ is the separation distance between two points on the phase front transverse to the axis of propagation and $J_0(\bullet)$ is the zero-order Bessel function.

By expanding the zero-order Bessel function in power series, the WSF is written in the form

$$D_{\mathrm{pl}}(\boldsymbol{\rho}, L) = A \sum_{n=1}^{\infty} \frac{(-1)^{n-1}\rho^{2n}}{(n!)^2 2^{2n}} \int_0^\infty \kappa^{2n-\frac{8}{3}} \left[1 + g\kappa^{\frac{2}{3}}\right] \left(w^2 e^{-a\kappa^{\frac{4}{3}} - b\kappa^2} + e^{-c\kappa^{\frac{4}{3}} - d\kappa^2} - 2we^{-e\kappa^{\frac{4}{3}} - f\kappa^2}\right) \mathrm{d}\kappa, \tag{9}$$

where the power spectrum given by Eq. (1) is used and the order of summation and integration is interchanged. In addition, $a = 8.284A_T\eta^{4/3}$, $b = 12.978A_T\eta^2$, $c = 8.284A_S\eta^{4/3}$, $d = 12.978A_S\eta^2$,

$e = 8.284A_{TS}\eta^{4/3}$, $f = 12.978A_{TS}\eta^2$, $g = 2.35\eta^{2/3}$ and $A = 8\pi^2k^2\left(0.388\times10^{-8}\right)\varepsilon^{-1/3}\chi_T/w^2$ are taken in Eq. (9).

Based on the properties of hypergeometric function and Pochhammer symbol [14], after very tedious calculations [10], the WSF of a plane wave in certain asymptotic regimes is

$$D_{\mathrm{pl}}(\rho,L)\approx\begin{cases}3.063\times10^{-7}k^2L\varepsilon^{-1/3}\dfrac{\chi_T}{w^2}\rho^2\left(16.958w^2-44.175w+118.923\right), (\rho\ll\eta)\\ 3.063\times10^{-7}k^2L\varepsilon^{-1/3}\dfrac{\chi_T}{w^2}\rho^{5/3}\left(1.116w^2-2.235w+1.119\right), \quad (\rho\gg\eta)\end{cases}. \tag{10}$$

The separation distance at which the modulus of the complex degree of coherence (DOC) falls to $1/e$ defines the spatial coherence radius ρ_0, that is, $D(\rho_0,L)=2$. Based on the expressions given in Eq. (10), the plane-wave spatial coherence radius can be expressed as

$$\rho_{0\mathrm{pl}}\approx\begin{cases}\left[3.063\times10^{-7}k^2L\varepsilon^{-1/3}\frac{\chi_T}{2w^2}\left(16.958w^2-44.175w+118.923\right)\right]^{-1/2}, (\rho_0\ll\eta)\\ \left[3.063\times10^{-7}k^2L\varepsilon^{-1/3}\frac{\chi_T}{2w^2}\left(1.116w^2-2.235w+1.119\right)\right]^{-3/5}, \quad (\rho_0\gg\eta)\end{cases}. \tag{11}$$

3.2. Spherical wave

Under Rytov approximation, the WSF of a spherical wave is defined by [1].

$$D_{\mathrm{sp}}(\rho,L)=8\pi^2k^2L\int_0^1\int_0^\infty[1-J_0(\kappa\xi\rho)]\Phi_n(\kappa)\kappa\mathrm{d}\kappa\mathrm{d}\xi, \tag{12}$$

Similarly, the WSF of a spherical wave is derived in [10].

$$D_{\mathrm{sp}}(\rho,L)\approx\begin{cases}3.063\times10^{-7}k^2L\varepsilon^{-1/3}\dfrac{\chi_T}{w^2}\rho^2\left(5.623w^2-14.725w+39.641\right), (\rho\ll\eta)\\ 3.063\times10^{-7}k^2L\varepsilon^{-1/3}\dfrac{\chi_T}{w^2}\rho^{5/3}\left(0.419w^2-0.838w+0.419\right), (\rho\gg\eta)\end{cases}, \tag{13}$$

and the spherical-wave spatial coherence radius as [10].

$$\rho_{0\mathrm{sp}}\approx\begin{cases}\left[3.603\times10^{-7}k^2L\varepsilon^{-1/3}\frac{\chi_T}{2w^2}\left(5.623w^2-14.725w+39.641\right)\right]^{-1/2}, (\rho_0\ll\eta)\\ \left[3.603\times10^{-7}k^2L\varepsilon^{-1/3}\frac{\chi_T}{2w^2}\left(0.419w^2-0.838w+0.419\right)\right]^{-3/5}, (\rho_0\gg\eta)\end{cases}. \tag{14}$$

3.3. Discussions

Based on the formula of Eqs. (10), (11), (13), and (14), the WSF of both a plane wave and a spherical wave can be written as

$$D(\rho,L)=\begin{cases}2(\rho/\rho_0)^2, & (\rho\ll\eta)\\ 2(\rho/\rho_0)^{5/3}, & (\rho\gg\eta)\end{cases}. \tag{15}$$

Equation (15) indicates that the spatial coherence radius is the only parameter characterizing

the WSF, and under Rytov approximation, the Kolmogorov five-thirds power law of wave structure function is valid for oceanic turbulence in the inertial range if the power spectrum of oceanic turbulence proposed by Nikishov is adopted.

According to Ref. [1], under Rytov approximation, the definitions of wave structure function of a plane wave and a spherical wave are given by Eqs. (8) and (12), respectively. It is known that the expression for wave structure function depends on the mutual coherence function. Rytov approximation is limited to weak fluctuations. However, for the special cases of a plane wave and a spherical wave, it has been shown that mutual coherence function derived by strong fluctuation theories is the same as that derived by Rytov approximation [1]. Only a plane-wave and a spherical-wave case are considered in this section. Thus, the results of the wave structure function and the spatial coherence radius obtained are valid in both weak and strong fluctuations.

4. Angle-of-arrival fluctuations

Angle-of-arrival (AOA) fluctuations play an important role in a diverse range of fields including atmospheric turbulence [15, 16], free space optical communication [17], ground-based astronomical observations [18], and so on.

Angle-of-arrival fluctuations of an optical wave in the plane of the receiver aperture are associated with image dancing in the focal plane of an imaging system. Fluctuations in the AOA can be described in terms of the phase structure function [1]. In order to understand it easily, let ΔS denote the total phase shift across a collecting lens of diameter $2W_G$ and Δl the corresponding optical path difference. These quantities are related to [1]

$$k\Delta l = \Delta S, \tag{16}$$

Under the geometrical optics method, the AOA is defined by [19].

$$\beta_a = \frac{\Delta l}{2W_G} = \frac{\Delta S}{2kW_G}, \tag{17}$$

Based on the homogeneous and isotropic oceanic turbulence, the mean $\langle \beta_a \rangle = 0$ will be satisfied. The variance of AOA can be expressed as [1].

$$\langle {\beta_a}^2 \rangle = \frac{\left\langle (\Delta S)^2 \right\rangle}{(2kW_G)^2} = \frac{D_S(2W_G, L)}{(2kW_G)^2}, \tag{18}$$

where $D_S(\rho, L)$ is the phase structure function with the radial distance $\rho = 2W_G$.

4.1. Angle-of-arrival fluctuations of plane wave

The phase structure function associated with an unbounded plane wave is given by [1].

$$D_{S\text{-pl}}(\boldsymbol{\rho}, L) = 4\pi^2 k^2 L \int_0^1 \int_0^\infty \kappa \Phi_n(\kappa)[1 - J_0(\kappa\boldsymbol{\rho})]\left[1 + \cos\left(\frac{L\kappa^2\xi}{k}\right)\right] \mathrm{d}\kappa \mathrm{d}\xi, \tag{19}$$

where the normalized distance variable $\xi = 1 - z/L$.

Based on Eqs. (18) and (19), the AOA fluctuations for a plane wave can be expressed as [1].

$$\left\langle \beta_a^2 \right\rangle_{\text{pl}} = \frac{D_{S\text{-pl}}(2W_G, L)}{(2kW_G)^2}, \tag{20}$$

the variance of AOA in the $\rho \gg \eta$ case is presented in this section; therefore, $\rho \gg (L/k)^{1/2}$ and the geometrical optics approximation $L\kappa^2/k \ll 1$ is satisfied.

By using $\cos\left(L\kappa^2\xi/k\right) \approx 1 - L^2\kappa^4\xi^2/2k^2$ and after very tedious calculations [20], the phase structure function of a plane wave in the inertial range as,

$$\begin{aligned} D_{S\text{-pl}}(\boldsymbol{\rho}, L) \approx \varepsilon^{-1/3}\left(\chi_T/w^2\right)\rho^{5/3}[3.063 \times 10^{-7}k^2 L\left(1.116w^2 - 2.235w + 1.119\right) \\ - L^3\left(1.841w^2 - 40.341w + 2077\right)], \qquad (\rho \gg \eta) \end{aligned} \tag{21}$$

Substituting Eq. (21) into Eq. (20), the analytical expression of AOA fluctuations for a plane wave is

$$\begin{aligned} \left\langle \beta_a^2 \right\rangle_{\text{pl}} \approx \varepsilon^{-1/3}\left(\chi_T/w^2\right)(2W_G)^{-1/3}[3.063 \times 10^{-7}k^2 L\left(1.116w^2 - 2.235w + 1.119\right) \\ - L^3\left(1.841w^2 - 40.341w + 2077\right)], \qquad (2W_G \gg \eta) \end{aligned} \tag{22}$$

To clarify the physical explanation, we introduce the plane-wave spatial coherence radius $\rho_{0\text{pl}}$ (see Ref. [10] in the inertial range) in Eqs. (21) and (22), and the simplified expressions of phase structure function and AOA fluctuations for plane waves can be expressed as

$$D_{S\text{-pl}}(\boldsymbol{\rho}, L) \approx C_1\left(\frac{\rho}{\rho_{0\text{pl}}}\right)^{5/3}, \qquad (\rho \gg \eta) \tag{23}$$

$$\left\langle \beta_a^2 \right\rangle_{\text{pl}} \approx 2C_1 k^{-2}(2W_G)^{-1/3}{\rho_{0\text{pl}}}^{-5/3}, \qquad (2W_G \gg \eta) \tag{24}$$

where $C_1 = 2\left[1 - L^2\left(1.84w^2 - 40.341w + 2077\right)/3.063 \times 10^{-7}k^2\left(1.116w^2 - 2.235w + 1.119\right)\right]$.

4.2. Angle-of-arrival fluctuations of a spherical wave

In the case of a spherical wave, the phase structure function is defined by [1].

$$D_{S\text{-sp}}(\boldsymbol{\rho}, L) = 4\pi^2 k^2 L \int_0^1 \int_0^\infty \kappa \Phi_n(\kappa)[1 - J_0(\kappa\boldsymbol{\rho})]\left\{1 + \cos\left[\frac{L\kappa^2\xi(1-\xi)}{k}\right]\right\} \mathrm{d}\kappa \mathrm{d}\xi, \tag{25}$$

Based on Eq. (25), the AOA fluctuations for a spherical wave can be written as [1].

$$\left\langle \beta_a^2 \right\rangle_{\text{sp}} = \frac{D_{S\text{-sp}}(2W_G, L)}{(2kW_G)^2}, \tag{26}$$

Similarly, the phase structure function of a spherical wave is expressed as

$$\begin{aligned} D_{S\text{-sp}}(\rho, L) \approx \varepsilon^{-1/3}\left(\chi_T/w^2\right)\rho^{5/3}[3.063 \times 10^{-7}k^2L\left(0.4196w^2 - 2.235w + 0.419\right) \\ - L^3\left(0.184w^2 - 4.034w + 207.7\right)], \qquad (\rho \gg \eta) \end{aligned} \tag{27}$$

and the analytical expression of AOA fluctuations for a spherical wave is

$$\begin{aligned} \left\langle \beta_a^2 \right\rangle_{\text{sp}} \approx \varepsilon^{-1/3}\left(\chi_T/w^2\right)(2W_G)^{-1/3}[3.063 \times 10^{-7}k^2L\left(0.4196w^2 - 2.235w + 0.419\right) \\ - L^3\left(0.184w^2 - 4.034w + 207.7\right)], \qquad (2W_G \gg \eta). \end{aligned} \tag{28}$$

Substituting the spherical-wave spatial coherence radius $\rho_{0\text{sp}}$ (see Ref. [10]) in Eqs. (27) and (28), phase structure function and AOA fluctuations for the spherical wave are

$$D_{S\text{-sp}}(\rho, L) \approx C_2\left(\frac{\rho}{\rho_{0\text{sp}}}\right)^{5/3}, \qquad (\rho \gg \eta) \tag{29}$$

$$\left\langle \beta_a^2 \right\rangle_{\text{sp}} \approx 2C_2k^{-2}(2W_G)^{-1/3}{\rho_{0\text{sp}}}^{-5/3}, \qquad (2W_G \gg \eta) \tag{30}$$

where $C_2 = 2\left[1 - L^2\left(0.184w^2 - 4.034w + 207.7\right)/3.063 \times 10^{-7}k^2\left(0.419w^2 - 0.838w + 0.419\right)\right]$.

4.3. Discussions

As mentioned in Section 1, the spatial coherence radius plays an important role in a heterodyne detection system. To the best of our knowledge, it is interesting to research the relation between AOA fluctuations and the spatial coherence radius, because spatial coherence radius ρ_0 represents the coherence degradation of laser beams propagating through ocean induced by the strength of turbulence. Both for plane-wave and for spherical-wave models, it is shown that AOA is inversely proportional to five-thirds order of spatial coherence radius in the inertial range. Besides, the difference of AOA fluctuations between an atmospheric turbulence and an oceanic turbulence is that the constant $C_i(i = 1, 2)$ occurs in the analytical expressions of AOA fluctuations in the latter one. Due to the constant C_i related to wavelength, propagation distance, and oceanic parameters, changes of oceanic parameter on constant C_i are investigated at fixed wavelength and propagation path [20]. To illustrate this case, $w = -1$ (i.e., $C_1 = 1.966$, $C_2 = 1.991$) is chosen in the theoretical calculations, and it is clear that constant C_i approximates to 2 both for plane and for spherical waves; thus, Eqs. (24) and (30) are consistent with the expressions of AOA fluctuations in atmospheric turbulence. In Ref. [20], changes of AOA fluctuations versus ρ_0 (i.e., $\rho_{0\text{pl}}$ in a plane-wave case and $\rho_{0\text{sp}}$ for a spherical-wave model, respectively) are illustrated in **Figure 1**. Both for a plane wave and for a spherical wave, AOA fluctuations decrease as ρ_0 increases. It is clear that AOA fluctuations have a

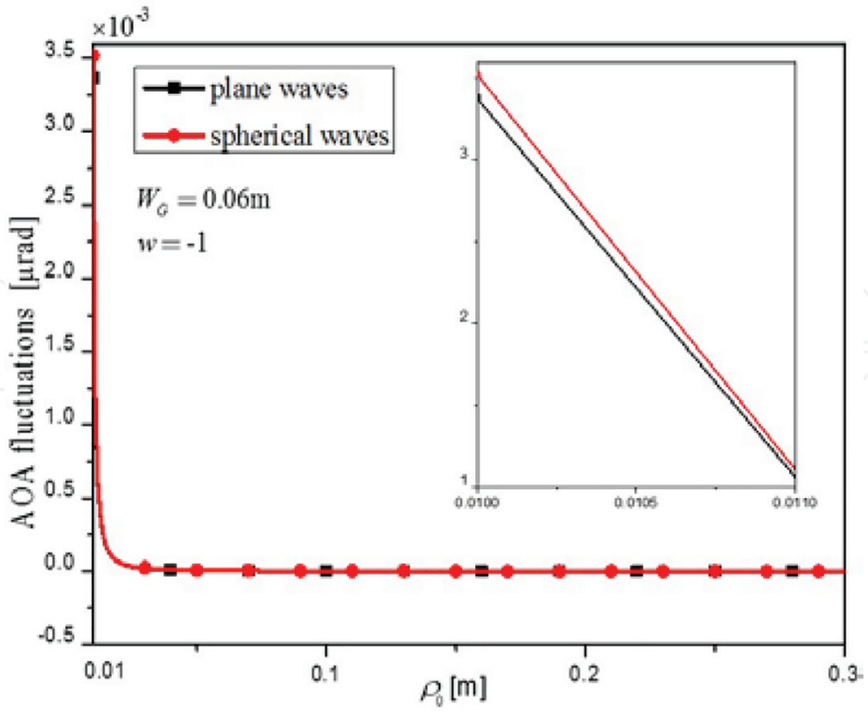

Figure 1. Changes of AOA fluctuations for oceanic turbulence versus ρ_0 in two models [20].

smaller value when the larger spatial coherence radius is obtained, and the AOA fluctuations of a spherical wave are larger than that of a plane wave at the fixed ρ_0. In terms of the influences of spatial coherence radius, the AOA fluctuations of plane and spherical waves in oceanic turbulence have the similar behavior to that of atmospheric turbulence.

5. Beam wander

Movement of the short-term beam instantaneous center (or "hot spot") is commonly called beam wander [1]. This phenomenon can be characterized statistically by the variance of the hot spot displacement along an axis or by the variance of the magnitude of the hot spot displacement [1]. An estimate of the short-term beam radius is obtained by removing beam wander effects from the long-term beam radius [1]. It is much convenient to use the geometrical optics approximation method in the turbulent area. Beam wander is an important characteristic of laser beams, which determines their utility for practical applications, such as ground-to-satellite laser communication [2, 3] and global quantum communication [4].

5.1. A general model

The far-field angular spread of a free-space propagating beam of diameter $2W_0$ is of order $\lambda/2W_0$. In the presence of optical turbulence, a finite optical beam will experience random deflections as it propagates, causing further spreading of the beam by large-scale inhomogeneities of the turbulence [1]. Over short time periods, the beam profile at the receiver moves off

the bore sight and can become highly skewed from Gaussian so that the instantaneous center of the beam is randomly displaced [1]. According to Ref. [1], W^2T_{LS} describes the beam wander or the variance of the instantaneous center of the beam in the receiver plane ($z = L$).

Based on the introduction of a general model [1], beam wander can be expressed as

$$\begin{aligned}\left\langle r_c^2\right\rangle &= W^2T_{LS}\\ &= 4\pi^2k^2W^2\int_0^L\int_0^\infty \kappa\Phi_n(\kappa)H_{LS}(\kappa,z)\left[1-\exp\left(-\Lambda L\kappa^2\xi^2/k\right)\right]\mathrm{d}\kappa\mathrm{d}z,\end{aligned} \tag{31}$$

where bracket < > denotes an ensemble average, W is the beam radius in the free space at receiver, Λ represents Fresnel ration of beam at receiver, and $H_{LS}(\kappa, z)$ is the large-scale filter function, respectively.

The large-scale filter function is [1].

$$H_{LS}(\kappa,\xi) = \exp\left\{-\kappa^2W_0^2\left[\left(\Theta_0+\overline{\Theta}_0\xi\right)^2+\Lambda_0^2(1-\xi)^2\right]\right\}, \tag{32}$$

where $\Theta_0 = 1-\overline{\Theta}_0$. W_0, Θ_0 and Λ_0 are the beam radius, the beam curvature parameter, and Fresnel ration of beam at transmitter, respectively [1].

Because beam wander is caused mostly by a large-scale turbulence near the transmitter, the last term can be dropped in Eq. (32) and the geometrical optics approximation is [1].

$$1-\exp\left(-\Lambda L\kappa^2\xi^2/k\right) = \Lambda L\kappa^2\xi^2/k, \qquad L\kappa^2/k \ll 1. \tag{33}$$

Substituting from Eqs. (1), (32), and (33) into Eq. (31), (31) leads to

$$\begin{aligned}\left\langle r_c^2\right\rangle &= 0.388\times10^{-8}\times4\pi^2kW^2L\Lambda\varepsilon^{-1/3}\left(\chi_T/w^2\right)\\ &\times\int_0^1\int_0^\infty \kappa^{-2/3}\left[1+2.35(\kappa\eta)^{2/3}\right]\left[w^2\exp\left(-A_T\delta\right)+\exp\left(-A_S\delta\right)-2w\exp\left(-A_{TS}\delta\right)\right]\\ &\exp\left[-\kappa^2W_0^2\left(\Theta_0+\overline{\Theta}_0\xi\right)^2\right]\xi^2\mathrm{d}\kappa\mathrm{d}\xi\end{aligned}, \tag{34}$$

Equation (34) is applicable for collimated, divergent, or focused Gaussian-beam waves, and it can represent our general expression for the variance of beam wander displacement under weak irradiance fluctuations.

5.2. Special cases

In this section, two special cases (i.e., collimated beam and focused beam) are analyzed.

For collimated beam ($\Theta_0 = 1$), the beam wander can be simplified as

$$\left\langle r_c^2 \right\rangle_{coll} = 0.517 \times 10^{-8} \times \pi^2 k W^2 L \Lambda \varepsilon^{-1/3} \left(\chi_T / w^2\right) \left(\alpha w^2 - 2\beta w + \gamma\right), \tag{35}$$

where

$$\begin{aligned} \alpha = {} & 37.9244\eta^4 A_T^2 \left(W_0^2 + 12.978 A_T \eta^2\right)^{-11/6} + 15.2043\eta^{8/3} A_T^2 \left(W_0^2 + 12.978 A_T \eta^2\right)^{-3/2} \\ & - 9.03014\eta^{8/3} A_T \left(W_0^2 + 12.978 A_T \eta^2\right)^{-7/6} - 4.67544\eta^{4/3} A_T \left(W_0^2 + 12.978 A_T \eta^2\right)^{-5/6} \\ & + 2.08263\eta^{4/3} \left(W_0^2 + 12.978 A_T \eta^2\right)^{-1/2} + 2.78316 \left(W_0^2 + 12.978 A_T \eta^2\right)^{-1/6}. \end{aligned} \tag{36}$$

and β, γ can be obtained from Eq. (36) if A_T is replaced by A_{TS}, A_S, respectively.

For focused beam ($\Theta_0 = 0$), the beam wander is expressed as

$$\left\langle r_c^2 \right\rangle_{focu} = 0.517 \times 10^{-8} \times \pi^2 k W^2 L \Lambda \varepsilon^{-1/3} \left(\chi_T / w^2\right) \left(\alpha' w^2 - 2\beta' w + \gamma'\right), \tag{37}$$

where

$$\begin{aligned} \alpha' = \int_0^1 & 37.9244\eta^4 A_T^2 \left(W_0^2 \xi^2 + 12.978 A_T \eta^2\right)^{-11/6} + 15.2043\eta^{8/3} A_T^2 \left(W_0^2 \xi^2 + 12.978 A_T \eta^2\right)^{-3/2} \\ & - 9.03014\eta^{8/3} A_T \left(W_0^2 \xi^2 + 12.978 A_T \eta^2\right)^{-7/6} - 4.67544\eta^{4/3} A_T \left(W_0^2 \xi^2 + 12.978 A_T \eta^2\right)^{-5/6} \\ & + 2.08263\eta^{4/3} \left(W_0^2 \xi^2 + 12.978 A_T \eta^2\right)^{-1/2} + 2.78316 \left(W_0^2 \xi^2 + 12.978 A_T \eta^2\right)^{-1/6} \xi^2 \mathrm{d}\xi. \end{aligned} \tag{38}$$

and β', γ' can be obtained from Eq. (38) when A_T is replaced by A_{TS}, A_S, respectively.

To atmospheric turbulence, the focused beam case leads to a greater beam wander variance for the same size beam at the transmitter as that for the collimated beam [1]. However, because of the complexity of oceanic power spectrum, the analytical expressions of collimated beam and focused beam are also less concise than those of atmospheric turbulence. Therefore, it is not simple to distinguish whose variance of beam wander is the larger one directly. In Section 5.4, numerical calculations are used to discuss the abovementioned property of different beams.

5.3. Dimensionless quantity B_W

In order to obtain influences of beam wander on laser beam propagation through oceanic turbulence, the relation between beam wander and the turbulence-induced beam spot size is investigated in detail by using theoretical and numerical methods. Using the dimensionless quantity $B_W = \left\langle r_c^2 \right\rangle / W^2(1+T)$, where $T = 4\pi^2 k^2 L \int_0^1 \int_0^\infty \kappa \Phi_n(\kappa) \left(1 - e^{-\Lambda L \kappa^2 \xi^2 / k}\right) \mathrm{d}\kappa \mathrm{d}\xi$ [1]. Based on Ref. [21], the quantity in oceanic turbulence can be expressed as $T = 0.517 \times 10^{-8} \pi^2 k L^2 \Lambda \varepsilon^{-1/3} \chi_T \left(67.832 w^2 - 176.699 w + 475.692\right) / w^2$. For the dimensionless quantity, B_W is more informative than merely $\left\langle r_c^2 \right\rangle$ about the practical significance of the beam wander. The quantity B_W can be used to investigate the proportion of beam wander $\left\langle r_c^2 \right\rangle$ to the turbulence-induced beam spot size $W^2(1+T)$ [1]. In **Figure 2**, the dimensionless quantity B_W as a function of the three oceanic parameters is plotted. It is shown that the larger value of B_W is related to smaller

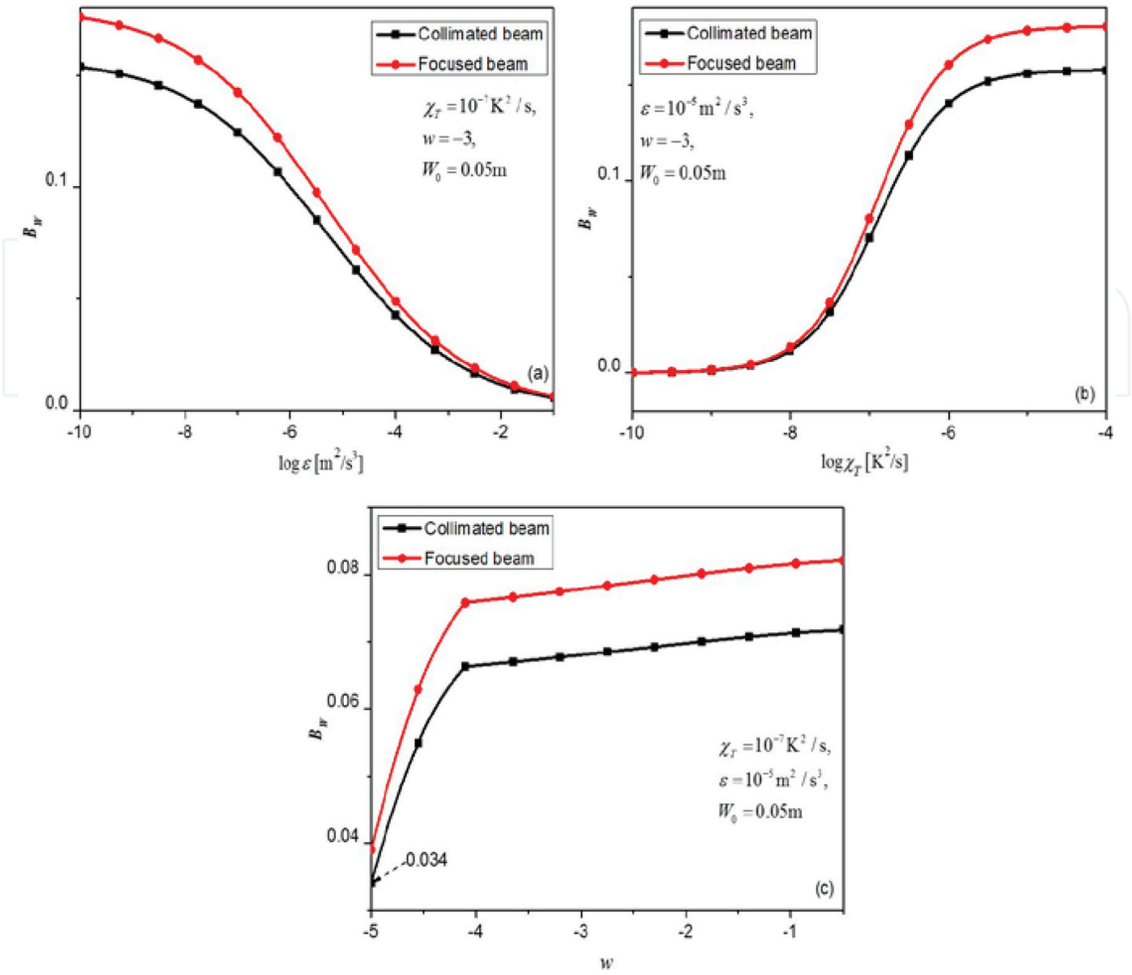

Figure 2. Dimensionless quantity B_W for collimated and focused beam versus (a) $\log\varepsilon$, (b) $\log\chi_T$ and (c) w [22].

$\log\varepsilon$, larger $\log\chi_T$, and salinity-induced dominant. The beam wander of collimated beam has less influence on turbulence-induced beam spot size compared to that of focused beam. Furthermore, beam wander plays an unignorable role in turbulence-induced beam spot size because all the values of B_W are larger than 0.034 (or 3.4%) shown in **Figure 2**. The beam wander effect cannot be ignored on laser beam propagating through ocean.

5.4. Definition of relative beam wander

To obtain the difference of beam wander among various beam types, the relative beam wander $\langle r_c^2\rangle_R$ based on focused and collimated beam is defined, which can be expressed as

$$\begin{aligned}\langle r_c^2\rangle_R &= \langle r_c^2\rangle_{focu} - \langle r_c^2\rangle_{coll} \\ &= 0.517\times10^{-8}\times\pi^2 kW^2 L\Lambda\varepsilon^{-1/3}\left(\chi_T/w^2\right)\left[(\alpha'-\alpha)w^2 - 2(\beta'-\beta)w + (\gamma'-\gamma)\right].\end{aligned} \tag{39}$$

It is clear that the increment $\langle r_c^2\rangle_R' = \langle r_c^2\rangle_{focu} - \langle r_c^2\rangle_{arbi}$ or $\langle r_c^2\rangle_R' = \langle r_c^2\rangle_{arbi} - \langle r_c^2\rangle_{coll}$ of arbitrary beam type (i.e., $0 < \Theta_0 < 1$) is smaller than that of Eq. (39). Choosing the same turbulent

strength and beam radius (i.e., $\varepsilon = 10^{-5}\mathrm{m}^2/\mathrm{s}^3$, $\chi_T = 10^{-7}\mathrm{K}^2/\mathrm{s}$, $w = -3$ and $W_0 = 0.05\mathrm{m}$) shown in **Figure 3**, the value of $\langle r_c^2 \rangle_R / \langle r_c^2 \rangle_{focu}$ is equal to 0.124. For arbitrary beam, it is clear that the ratio of $\langle r_c^2 \rangle_R' / \langle r_c^2 \rangle_{focu}$ is smaller than 0.124. The extension to arbitrary oceanic parameters and beam radius is straightforward.

From Section 5.3, it is impossible to avoid the beam wander effect for laser propagation; therefore, achieving small beam wander is imperative. In this section, the relative beam wander describes the increment of beam wander between focused and collimated beam, and this quantity benefits us to select how to obtain small value of beam wander. Based on Eq. (39), it is feasible to obtain small beam wander as long as the arbitrary beam type is under $\Theta_0 \to 1$ condition. **Figure 3** shows that the larger beam radius leads to a smaller value of beam wander. In the practical applications, it is an effective feasible solution to achieve a small beam wander effect when beam curvature parameter at transmitter Θ_0 is approximate to 1 and beam radius is appropriately large. It is also meaningful to select favorable beam parameters which are less sensitive to turbulence in laser propagation applications.

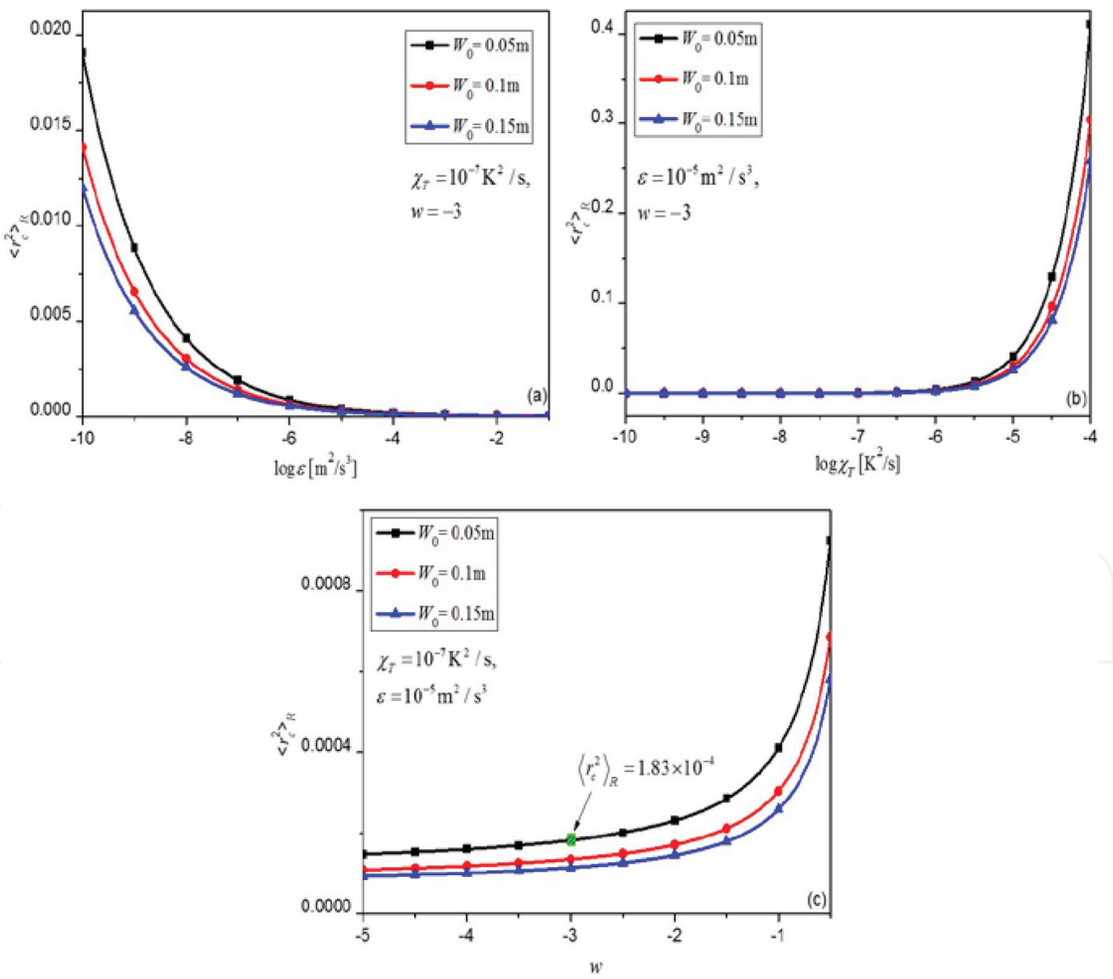

Figure 3. Relative beam wander with various beam radii versus (a) $\log\varepsilon$, (b) $\log\chi_T$ and (c) w [22].

6. Conclusions

In summary, this chapter has used the same idea to convert atmospheric turbulence concerning beam wave propagation to corresponding oceanic turbulence. The general characteristics of an optical wave propagating through the ocean are greatly affected by small fluctuations in the refractive index that are the direct consequence of small temperature and salinity fluctuations transported by the turbulent motion of the ocean. Therefore, the propagation process of one optical wave suffers beam spreading, loss of spatial coherence, angle-of-arrival fluctuations, beam wander, and so on. In this chapter, three important statistical quantities including spatial coherence radius, angle-of-arrival fluctuations, and beam wander have been investigated.

The analytical formulae for the wave structure function and the spatial coherence radius of a plane wave and a spherical wave propagating through oceanic turbulence have been derived in Section 3, which are valid in both weak and strong fluctuations. It has been shown that under Rytov approximation, the Kolmogorov five-thirds power law of wave structure function is also valid for the oceanic turbulence in the inertial range if the power spectrum of oceanic turbulence proposed by Nikishov is adopted. These results are of considerable theoretical and practical interest for operations in communication, imaging, and sensing systems involving turbulent underwater channels.

Furthermore, spatial coherence radius can be described as the coherence degradation of laser beams propagating through ocean induced by the strength of turbulence; thus, the relation between angle-of-arrival fluctuations and the spatial coherence radius has been researched. Both for a plane wave and for a spherical wave, it is shown that the angle-of-arrival fluctuations are inversely proportional to five-thirds order of spatial coherence radius in the inertial range. In terms of the influences of spatial coherence radius, the angle-of-arrival fluctuations of plane and spherical waves in oceanic turbulence have the similar behavior to that of atmospheric turbulence.

In addition, based on the oceanic power spectrum, the beam wander effect has been studied with analytical and numerical methods in weak fluctuation theory, and the analytical expressions for beam wander of collimated and focused beam in oceanic turbulence have also been derived. For the dimensionless quantity, B_W, the relation between beam wander and the turbulence-induced beam spot size has been investigated. It is shown that the beam wander of collimated beam has less influence on turbulence-induced beam spot size compared to that of focused beam. Particularly, according to the definition of the relative beam wander, it is shown that the relative beam wander is small when the value of beam curvature parameter at transmitter Θ_0 is close to 1 (i.e., $\Theta_0 \to 1$) and beam radius W_0 is properly large.

In this chapter, the classical treatments of optical wave propagation have been concerned with part of special cases, such as uniform plane wave, spherical wave, collimated beam, and focused beam. The results presented serve as a foundation for the study of optical beam propagation in oceanic turbulence, which may provide an essential support for further researches in applications for underwater communicating, imaging, and sensing systems. Thus, these simple optical wave models are useful in describing certain aspects of wave

propagation in oceanic turbulence. However, due to inherent infinite extent, these models are not adequate in describing laser beams when finite size of the transmitted wave and high-order Gaussian wave should be taken into account in the near future.

Acknowledgements

Lu Lu and Zhiqiang Wang wrote this manuscript. Lu Lu, Zhiqiang Wang, and Chengyu Fan arranged the structure of this manuscript. Lu Lu and Xiaoling Ji performed theoretical calculations and physical analysis in Section 2. Lu Lu, Zhiqiang Wang, Pengfei Zhang, Chunhong Qiao, Jinghui Zhang, and Chengyu Fan performed Sections 3–5. Lu Lu deduced the analytical expressions. Zhiqiang Wang and Pengfei Zhang performed the numerical simulations and analyzed data. Pengfei Zhang, Jinghui Zhang, Chunhong Qiao, and Chengyu Fan revised this manuscript. All authors contributed this work equally and acknowledged the support by the National Natural Science Foundation of China (NSFC) under grants 61405205 and 61475105.

Conflict of interest

The authors declare no conflict of interest.

Notes

All authors are very much thankful to the valuable suggestions in the spatial coherence radius section by Prof. Yahya Baykal.

Author details

Zhiqiang Wang [1,2], Lu Lu [3*], Pengfei Zhang [1], Chunhong Qiao [1*], Jinghui Zhang [1], Chengyu Fan [1*] and Xiaoling Ji [4]

*Address all correspondence to: lulu19900101@berkeley.edu; chqiao@aiofm.ac.cn; cyfan@aiofm.ac.cn

1 Key Laboratory of Atmospheric Optics, Anhui Institute of Optics and Fine Mechanics, Chinese Academy of Sciences, Hefei, China

2 University of Science and Technology of China, Hefei, China

3 University of California, Berkeley, CA, USA

4 Department of Physics, Sichuan Normal University, Chengdu, China

References

[1] Andrews LC, Phillips RL. Laser Beam Propagation Through Random Media. 2nd ed. Bellingham: SPIE; 2005

[2] Dios F, Rubio JA, Rodríguez A, Comerón A. Scintillation and beam-wander analysis in an optical ground station-satellite uplink. Applied Optics. 2004;**43**:3866-3873. DOI: 10.1364/AO.43.003866

[3] Guo H, Luo B, Ren Y, Zhao S, Dang A. Influence of beam wander on uplink of ground-to-satellite laser communication and optimization for transmitter beam radius. Optics Letters. 2010;**35**:1977-1979. DOI: 10.1364/OL.35.001977

[4] Vasylyev DY, Semenov AA, Vogel W. Toward global quantum communication: Beam wandering preserves nonclassicality. Physical Review Letters. 2012;**108**:220501. DOI: 10.1103/PhysRevLett.108.220501

[5] Rothschild BJ, editor. Toward a Theory on Biological-Physical Interactions in the World Ocean. NATO ASI Series (Series C: Mathematical and Physical Sciences). Vol. 239. Dordrecht: Springer; 1988. pp. 215-234. DOI: 10.1007/978-94-009-3023-0_1

[6] Thorpe SA. An Introduction to Ocean Turbulence. Cambridge: Cambridge University Press; 2007

[7] Ferrari R, McWilliams JC, Canuto VM, Dubovikov M. Parameterization of Eddy fluxes near oceanic boundaries. Journal of Climate. 2008;**21**:2770-2789. DOI: 10.1175/2007JCLI1510.1

[8] Nikishov VV, Nikishov VI. Spectrum of turbulent fluctuations of the sea-water refraction index. International Journal of Fluid Mechanics Research. 2000;**27**:82-98. DOI: 10.1615/InterJFluidMechRes.v27.i1.70

[9] Lu W, Liu L, Sun J. Influence of temperature and salinity fluctuations on propagation of partially coherent beams in oceanic turbulence. Journal of Optics A: Pure and Applied Optics. 2006;**8**:1052-1058. DOI: 10.1088/1464-4258/8/12/004

[10] Lu L, Ji XL, Baykal Y. Wave structure function and spatial coherence radius of plane and spherical waves propagating through oceanic turbulence. Optics Express. 2014;**22**(22): 27112-27122. DOI: 10.1364/OE.22.027112

[11] Farwell N, Korotkova O. Intensity and coherence properties of light in oceanic turbulence. Optics Communication. 2012;**285**(6):872-875. DOI: 10.1016/j.optcom.2011.10.020

[12] Pao YH. Structure of turbulent velocity and scalar fields at large wavenumbers. Physics of Fluids. 1965;**8**:1063-1075. DOI: 10.1063/1.1761356

[13] Landahl MT, Mollo-Christensen E. Turbulence and Random Processes in Fluid Mechanics. 2nd ed. Cambridge: Cambridge University Press; 1992. p. 10

[14] Andrews LC. Special Functions of Mathematics for Engineers. 3rd ed. Oxford: SPIE and Oxford University; 1998

[15] Hill RJ. Review of optical scintillation methods of measuring the refractive index spectrum, inner scale and surface fluxes. Waves in Random and Complex Media. 1992;**2**:179-201. DOI: 10.1088/0959-7174/2/3/001

[16] Vilcheck MJ, Reed AE, Burris HR, Scharpf WJ, Moore CI, Suite MR. Multiple methods for measuring atmospheric turbulence. Proceedings of SPIE. 2002;**4821**:300-309. DOI: 10.1117/12.450631

[17] Eyyuboglu HT, Baykal Y. Analysis of laser multimode content on the angle-of-arrival fluctuations in free-space optics access systems. Optical Engineering. 2005;**44**:056002. DOI: 10.1117/1.1905383

[18] Masciadri E, Vernin J, Bougeault P. 3D mapping of optical turbulence using an atmospheric numerical model. I. A useful tool for the ground-based astronomy. Astronomy and Astrophysics Supplement Series. 1999;**137**(1):185-202. DOI: 10.1051/aas:1999475

[19] Tatarskii VI. Wave propagation in a Turbulence Medium, trans. In: Silverman RA, editor. New York: McGraw-Hill; 1961

[20] Lu L, Wang ZQ, Zhang PF, Qiao CH, Fan CY, Zhang JH, Ji XL. Phase structure function and AOA fluctuations of plane and spherical waves propagating through oceanic turbulence. Journal of Optics. 2015;**17**:085610. DOI: 10.1088/2040-8978/17/8/085610

[21] Lu L, Zhang PF, Fan CY, Qiao CH. Influence of oceanic turbulence on propagation of a radial Gaussian beam array. Optics Express. 2015;**23**:2827-2836. DOI: 10.1364/OE.23.002827

[22] Lu L, Wang ZQ, Zhang PF, Zhang JH, Fan CY, Ji XL, Qiao CH. Beam wander of laser beam propagating through oceanic turbulence. Optik. 2016;**127**:5341-5346. DOI: 10.1016/j.ijleo.2016.01.190